Helium II thermal counterflow at large heat currents*

D. R. Ladner, R. K. Childers, and J. T. Tough

Department of Physics, The Ohio State University, Columbus, Ohio 43210

(Received 17 September 1975)

Data for the temperature and pressure differences produced by the thermal counterflow of helium II in long capillaries are given and shown to define a region of nonlinear flow distinct from that described by Vinen. We suggest a simple modification of the Vinen theory associated with a secondary flow in the normal fluid and in good agreement with our data. The critical heat current for the onset of the secondary flow is shown to define a stability region in analogy to second-order phase transitions.

Our measurements of the temperature and pressure gradients in He II thermal counterflow[1-3] have added to the recent experimental support[4-6] for the Vinen theory[7] of superfluid turbulence. We have shown that these data are consistent with a mutual friction force $\vec{F}_{sn}$ and a superfluid eddy viscosity η_s, both of which are simple functions of a homogeneous vortex line density L_0. Vinen has given theoretical expressions for both $\vec{F}_{sn}(L_0)$ and the dependence of L_0 on the relative velocity of the superfluid and normal fluid, $\vec{v} = \vec{v}_s - \vec{v}_n$. There is as yet no theoretical result for comparison with our empirical determination of $\eta_s(L_0)$.

As we have previously emphasized, there are *two* distinct nonlinear flow regions and two critical heat currents obvious in our thermal counterflow data, as can be seen from the example in Fig. 1. It is important to note that it is in the region between 2 and 3 in Fig. 1 where the above analysis in terms of the Vinen theory is applied. The purpose of the present paper is to examine the critical heat current at point 3 (which we shall call $\dot{Q}_c$) and the nature of the flow at higher heat currents. Our data can be used to exclude several explanations of this third flow region, while at the same time they provide support for a rather simple physical model which we introduce.

A previous attempt[8] to understand $\dot{Q}_c$ and the dissipation for $\dot{Q} > \dot{Q}_c$ required combining data from several sources. This led to some erroneous conclusions, although the model suggested below bears some similarity to the previous one. In particular, we suggest that $\dot{Q}_c$ marks the onset of a secondary flow in the normal fluid and that the critical value of a normal-fluid Reynolds number depends on the vortex line density L_0. The third flow region ($\dot{Q} > \dot{Q}_c$) can then be understood quantitatively in terms of a simple modification of the Vinen theory, allowing for a new vorticity generation term arising from the secondary flow.

Our data were obtained with the apparatus described in detail elsewhere[3] and shown schematically in the inset to Fig. 1. Heat produced in the

heater reservoir is transferred through the helium in the flow tube to the temperature-regulated bath. The temperature and pressure differences ΔT and ΔP are detected by the resistance thermometer and pressure transducer and are displayed simultaneously on X-Y recorders as functions of the heat current $\dot{Q}$. Typical data emphasizing the third flow region are shown in Fig. 2. Data were obtained with a glass flow tube of diameter $d = 1.29 \times 10^{-2}$ cm and length $l = 10$ cm (tube 8 in Ref. 3). In order to further reveal the considerable detail in the ΔT data near $\dot{Q}_c$ we have employed the following technique: after $\dot{Q}$ is rapidly changed by a small amount, the temperature of pressure dif-
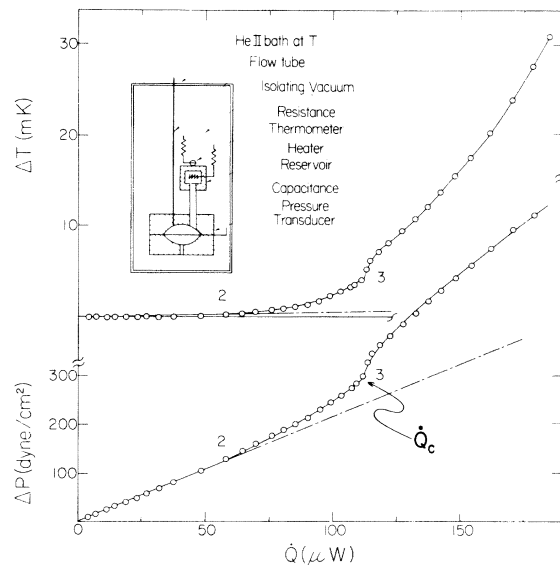

FIG. 1. Temperature- and pressure-difference data as a function of heat current $\dot{Q}$ obtained at $T = 1.7$ K and representative of other temperatures. The solid line is a guide to the eye and the broken line is an extrapolation of the linear region to higher heat currents. Points 2 and 3 are discussed in the text, as is the critical heat current $\dot{Q}_c$ at 3. Inset is a schematic drawing of the apparatus.
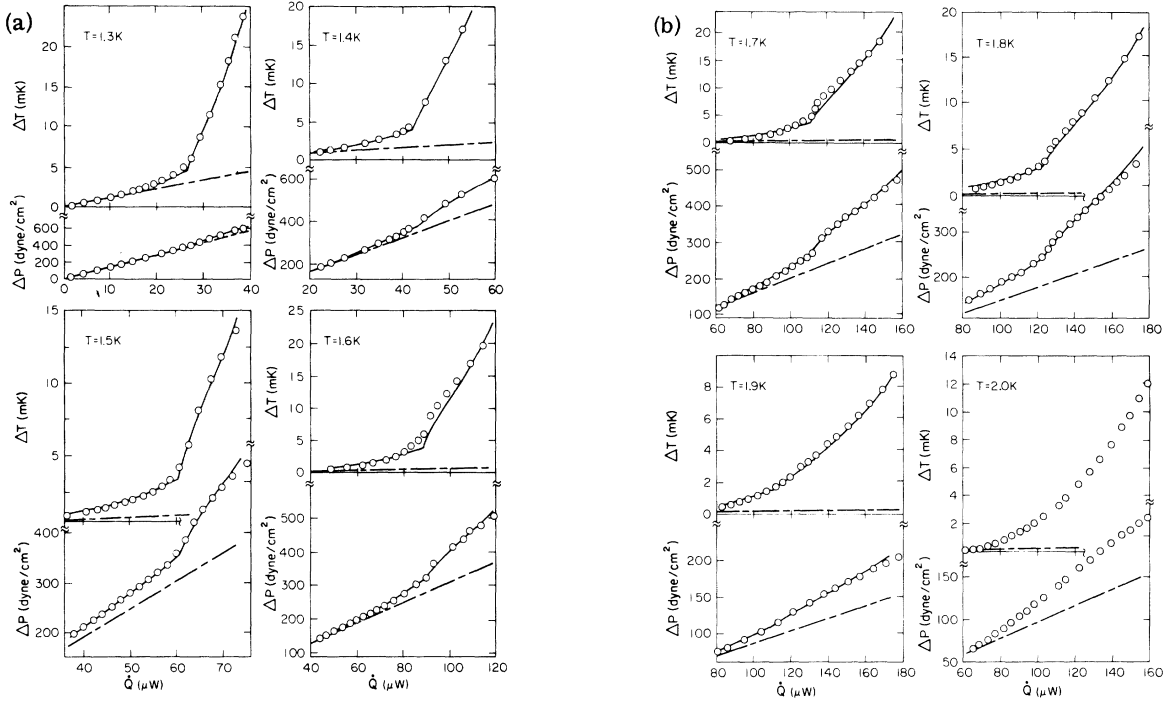
FIG. 2. (a) Temperature and pressure differences at $T = 1.3$ to 1.6 K as functions of the heat current $\dot{Q}$, emphasizing the data at high heat currents. The broken line is an extrapolation of the linear, low-$\dot{Q}$ region. The solid line is computed from the theory given in the text. Note that the zeros are often suppressed. (b) The temperature and pressure differences at $T = 1.7$ to 2.0 K as functions of the heat current $\dot{Q}$, emphasizing the data at high heat currents. The broken line is an extrapolation of the linear, low-$\dot{Q}$ region. The solid line is computed from the theory given in the text and is omitted at $T = 2.0$ K because the Vinen parameter χ_2 is not known there. Note that the zeros are often suppressed.

ference approaches its new equilibrium value as $1 - e^{-t/\tau}$. From measurements below $\dot{Q}_c$ we have verified that the experimental relaxation time τ is given by its theoretical value rC. The dynamic thermal resistance r is $d\Delta T/d\dot{Q}$, and the heat capacity C of the heater reservoir is dominated by the heat capacity of the helium it contains. The data for τ thus give the derivative of the ΔT vs $\dot{Q}$ curve. Figure 3 shows some of our data for τ and for corresponding ΔT obtained by direct integration of τ. It is clear from these results that there is a great deal of structure near $\dot{Q}_c$.

In our view, an analysis of the third flow region must begin with a proper set of dynamical equations for the preceding mutual friction region. We write these equations in the form

$$\vec{\nabla}P = \eta_n\nabla^2\vec{v}_n^{\,av} + \eta_s(L_0)\nabla^2\vec{v}_s^{\,av}, \tag{1}$$

$$\vec{\nabla}\mu = \vec{F}_{sn}(L_0) + \eta_s(L_0)\nabla^2\vec{v}_s^{\,av}, \tag{2}$$

where the chemical potential gradient is

$$\vec{\nabla}\mu = \vec{\nabla}P/\rho - S\vec{\nabla}T. \tag{3}$$

Here ρ is the total density of the fluid, S is the entropy per gram, η_n is the normal fluid viscosity, and $\vec{v}_n^{\,av}$ and $\vec{v}_s^{\,av}$ are the microscopically time-

averaged velocities of the normal fluid and superfluid as described in Ref. 3. The relative velocity $\vec{v}$ is uniform across the tube and is of magnitude

$$v = 4\dot{Q}/\pi d^2\rho_s ST. \tag{4}$$

The spacial averages of $\vec{v}_n^{\,av}$ and $\vec{v}_s^{\,av}$ over the tube cross section are denoted by $\vec{V}_n$ and $\vec{V}_s$ and are related to v as

$$\vec{V}_s = -(\rho_n/\rho_s)\vec{V}_n = (\rho_n/\rho)\vec{v}, \tag{5}$$

where ρ_n and ρ_s are the normal and superfluid densitites. The dynamical equations must of course be supplemented by equations for $F_{sn}(L_0)$ and $\eta_s(L_0)$:

$$F_{sn}(L_0) = (B\rho_s\rho_n\kappa/3\rho)vL_0, \tag{6}$$

$$\eta_s(L_0) = \kappa\rho(L_0\lambda^2)^{2/3}, \tag{7}$$

where B is the mutual friction parameter of Hall and Vinen,[9] κ is the quantum of circulation, and λ is the empirical constant derived from our pressure data.[2] Finally, it is necessary to give the dependence of L_0 on the relative velocity. Neglecting wall effects (which are insignificant in the region near $\dot{Q}_c$), the Vinen theory gives the steady-state vortex generation rate to be
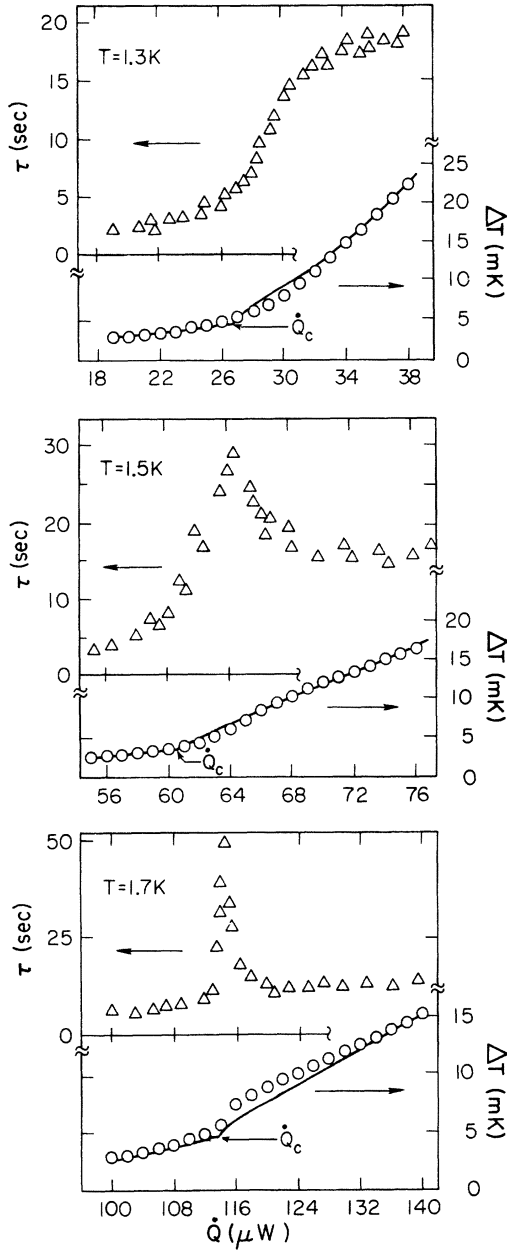
FIG. 3. Time constant for relaxation of ΔT or ΔP (triangles) as a function of $\dot{Q}$ near $\dot{Q}_c$, and the corresponding values of $\Delta T(\dot{Q})$ (circles) obtained by direct integration of a smooth curve drawn through the data. The solid lines on the ΔT data are calculated from the theory proposed in the text.

$$\dot{L}_g = (\chi_1 B \rho_n / 2\rho) v L_0^{3/2} \tag{8}$$

and the decay rate to be

$$\dot{L}_d = (\kappa \chi_2 / 2\pi) L_0^2 \tag{9}$$

giving an equilibrium line density

$$L_0^{1/2} = (\pi \chi_1 B \rho_n / \kappa \rho \chi_2) v . \tag{10}$$

Here χ_1 and χ_2 are the Vinen parameters given and discussed in Ref. 3. Equations (1)–(10) give an accurate description of the counterflow phenomena in the mutual friction region and we take them as our starting point for analysis of the third flow region.

Manipulation of Eqs. (1)–(3) quickly reveals that the excess temperature difference $\Delta T'$ is dominated by $\vec{F}_{sn}(L_0)$ and the excess pressure difference $\Delta P'$ is given solely by the $\eta_s(L_0)$ term. (By "excess" we mean the actual pressure or temperature difference minus the $L_0 = 0$ contribution.) In previous attempts to understand the third heat flow region, it was assumed that the normal fluid was turbulent and that Eq. (1) was modified by the addition of a force $\vec{F}_n$. While $\vec{F}_n$ can certainly be modeled to give the experimental $\Delta P'$ in this region, unless Eq. (2) is also modified in some way the resulting $\Delta T'$ is far less than what is observed. This is obvious when the domination of $\Delta T'$ by $\vec{F}_{sn}$ is recognized. Other possibilities that can also be discounted are modification of Eq. (6) (since this leaves $\Delta P'$ unaltered) and modification of Eq. (7) (since this cannot give a large enough $\Delta T'$). The only *single* modification that can possibly agree with our data is a change in the Vinen theory result in Eq. (10) for the equilibrium vortex line density. If for $\dot{Q} > \dot{Q}_c$ that result were replaced by

$$L_0^{1/2} = (\pi \chi_1 B \rho_n / \kappa \rho \chi_2) v + \Delta L_0^{1/2} , \tag{11}$$

then $\Delta T'$ and $\Delta P'$ would reflect this through $\vec{F}_{sn}$ and η_s, respectively. Using Eq. (11) and Eqs. (1)–(7) we have analyzed our data and found that indeed the *same* correction $\Delta L_0^{1/2}$ is needed for both the $\Delta T'$ and $\Delta P'$ data. This key experimental result means that the third heat flow region is simply one in which the vortex line density L_0 is modified from the value given by the Vinen theory, while the mutual fricition and eddy viscosity continue to depend on L_0 in the same way. The basic dynamical equations are thus left unchanged.

Without introducing another term in the dynamic balance of line generation and decay, it is impossible to modify the Vinen theory so that Eq. (11) results. Such a term was introduced by Vinen[10] to account for the inhomogeneity at the walls of the flow tube. In that case Vinen suggested that $\dot{L}_g$ be multiplied by a factor $(1 - \alpha / L_0^{1/2} d)$, where α is a constant of order unity and $L_0^{-1/2}$ is the mean spacing of vortex lines. We have demonstrated the success of this modification to the theory by an examination of the critical velocity introduced by it.[1] To account for $\Delta L_0^{1/2}$ in the third flow region we propose that the generation term again be modi-

fied, and that the source of the modification is a secondary flow in the normal fluid which commences at $\dot{Q}_c$. It is important to recall that in the Vinen region (between 2 and 3 in Fig. 1) the normal fluid is in Poiseuille flow only in a time-average sense. Because of the local mutual friction force, the actual normal fluid velocity field would find its classical analog in something like flow through a tube filled with a tangle of wire. The fact that classical Poiseuille flow is not unstable to a secondary flow (as is Couette flow to the formation of Taylor vortex cells, for example) does not necessarily preclude such an instability in the thermal counterflow probelm. Obviously there is no hint as to the structure of the postulated secondary flow, but there are some pertinent general results due to Landau.[11] In particular, he has shown that if the base flow becomes unstable at a critical Reynolds number R_c, then the velocity amplitude of the secondary flow increases as $\epsilon^{1/2}$, where $\epsilon \equiv (R - R_c)/R_c$ plays the role of an order parameter. This result, as well as other features of the Landau approach to hydrodynamic instabilities, has been confirmed in a number of experiments.[12,13]

Specifically, we propose that $\dot{Q}_c$ corresponds to a critical normal fluid Reynolds number above which a secondary flow of amplitude $v_0 \epsilon^{1/2}$ is present and that this flow modifies the Vinen vorticity generation term in the obvious manner

$$\dot{L}_g = (\chi_1 B \rho_n / 2\rho) v L_0^{1/2} \rightarrow (\chi_1 B \rho_n / 2\rho)(v + v_0 \epsilon^{1/2}) L_0^{1/2} .$$

(12)

This then leads to the result

$$\Delta L_0^{1/2} = (\pi \chi_1 B \rho_n / \rho \kappa \chi_2) v_0 \epsilon^{1/2} ,$$

(13)

where $\Delta L_0^{1/2}$ is defined in Eq. (11). Using this result we have fitted our ΔT and ΔP data for $\dot{Q} > \dot{Q}_c$ using v_0 as an adjustable parameter.[14] The results of this procedure are given by the solid lines in Fig. 2 and indicate excellent agreement with the data at all temperatures. It should be noted that the explicit dependence of $\Delta T'$ and $\Delta P'$ on $\dot{Q}$ and T as given by Eqs. (13), (11), (6), (7), (1), and (2) is extremely complex. There is a systematic deviation at the largest heat currents due to the very large temperature differences present there. We have not attempted to correct for this, although the correction would make the agreement even better. The values of $\dot{Q}_c$ used in this procedure are given in Table I.

In keeping with the terminology introduced by Vinen, we write the parameter v_0 in dimensionless form as

$$v_0 \equiv \chi_4 \kappa / \lambda .$$

(14)

Using $\lambda = 3 \times 10^{-5}$ cm, determined from the pres-

TABLE I. Values of the critical heat current $\dot{Q}_c$ and the parameter χ_4 defined in the text.

T (K)	$\dot{Q}_c$ (μW)	χ_4
1.3	27.0 ± 1.5	0.80 ± 0.02
1.4	42.5 ± 1.5	0.81 ± 0.02
1.5	60.5 ± 1.5	0.72 ± 0.03
1.6	88.5 ± 2.0	0.59 ± 0.03
1.7	111.0 ± 2.0	0.41 ± 0.04
1.8	123.0 ± 2.0	0.27 ± 0.03
1.9	110.0 ± 3.0	0.11 ± 0.02

sure data,[2] gives χ_4 as shown in Fig. 4 and given in Table I. While the temperature dependence of χ_4 is somewhat stronger than either χ_2 or B, it is encouraging to note that it is of the same order of magnitude.

Possible support for our proposed model may be found in measurements of the damping of a fine wire immersed in a thermal counterlow reported some years ago.[15] It was found that at low heat currents the damping was entirely due to the normal fluid viscosity, but that above a critical heat current there was an excess damping proportional to $\epsilon^{1/2}$. Possibly more significant, however, was the observation that this excess damping was anisotropic, being maximum for wire vibrations parallel to $\vec{V}_n$. These results are suggestive of a spacially periodic but time-independent secondary flow as described by Landau.[11]

One of the classic examples of secondary flows is the Taylor vortices which develop in the laminar flow between concentric rotating cylinders. Donnelly et al.[16] have demonstrated in an elegant experiment that the onset of the Taylor instability can be postponed substantially by modulation of the inner cylinder velocity at an appropriate frequency. Oberly and Tough[17] have observed an identical effect in thermal counterflow: the value of $\dot{Q}_c$ depended on the frequency of modulation of the normal-
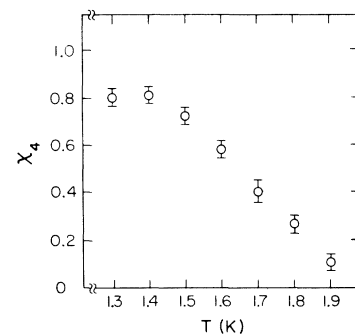

FIG. 4. Dimensionless parameter χ_4, defined in the text by Eq. (14), giving the amplitude of the proposed secondary flow as a function of temperature.

al fluid flow just as in the Taylor problem. These results were interpreted as evidence for the hydrodynamic origin of $\dot{Q}_c$, and we now suggest that they support our proposed model of a secondary flow.

The analogy between fluid instabilities and second-order phase transitions has often been made.[18] Both phenomena exhibit an order parameter which grows from zero in the neighborhood of a critical point, and both have a phase or stability boundary in the space of defining variables. Exploiting this analogy to phase transitions, we have examined the flow stability boundary corresponding to $\dot{Q}_c$. The state of the thermal counterflow can be defined by the vortex line density L_0 and a normal fluid Reynolds number, which for the present we choose as

$$R = \rho V_n d/\eta_n. \tag{15}$$

The analogy thus suggests that the R, L_0 plane should be separated into two regions in which the "Poiseuille" flow of the normal fluid is, respectively, stable and unstable to the formation of the secondary flow. The boundary between the two regions would then be $R_c(L_0)$, the critical Reynolds number. From our data we can construct $R_c(L_0)$, since at each temperature T both R and L_0 can be computed at $\dot{Q}_c$. Figure 5 gives the results of this calculation (the dimensionless quantity $L_0 d^2$ is used instead of L_0 here) and shows that the data do
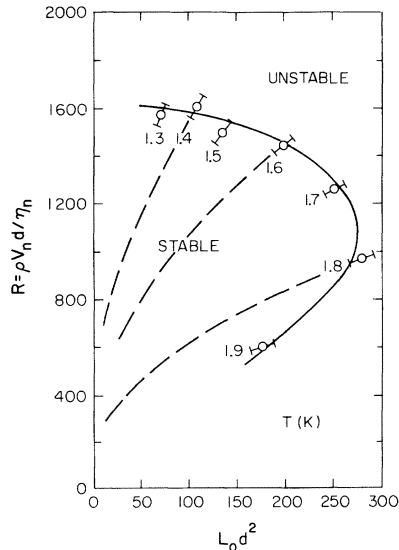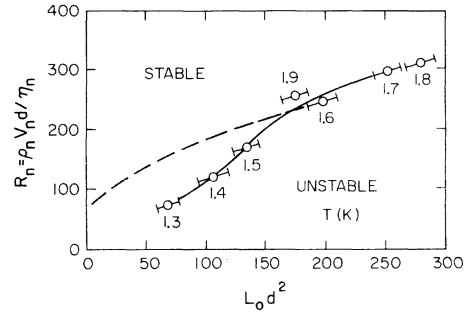

FIG. 6. Values of R_{nc} and $L_0 d^2$ determined from our data for $\dot{Q}_c$ at $T = 1.3$ to 1.9 K. The solid line, arbitrarily drawn through the data, divides the plane into regions which are stable and unstable to the formation of the proposed secondary flow. The dashed line represents the isotherm for $T = 1.6$ K.

fall along a reasonably smooth boundary in the plane. One might equally well choose the Reynolds number to be

$$R_n = \rho_n V_n d/\eta_n \tag{16}$$

in which case a similar calculation gives the results in Fig. 6. The dashed lines in Figs. 5 and 6 show several isotherms, the loci of points followed by the thermal counterflow at fixed temperatures as the heat current is varied.

In our experiments it is possible to increase the heat current in a smooth continuous fashion and observe the resulting temperature and pressure differences as functions of $\dot{Q}$ on X-Y recorders. In this way we often observe the linear region (Fig. 1) persisting to heat currents greater than $\dot{Q}_c$. However, if we begin this procedure with the flow in the mutual friction region, the third flow region *always* appears at $\dot{Q}_c$. These observations suggest the following: the flow transition at $\dot{Q}_c$ requires the presence of a high density of vortex lines, and the flow instability leading to the transition is with respect to infinitesimal rather than finite disturbances.

In conclusion, we have demonstrated that both temperature- and pressure-difference data obtained in thermal counterflow at large heat currents can be understood in terms of a simple modification of the Vinen theory. We suggest that the critical heat current $\dot{Q}_c$ marks the onset of a secondary flow in the normal fluid. Using the result that the amplitude of such a flow increases as $\epsilon^{1/2}$, we are able to obtain a satisfactory fit to our data. Other thermal counterflow experiments are shown to be supportive of our model. We point out the analogy between second-order phase transitions and flow instabilities and use our data to construct a stability diagram. Finally, we note that the existence of a highly correlated secondary flow

FIG. 5. Values of R_c and $L_0 d^2$ determined from our data for $\dot{Q}_c$ at $T = 1.3$ to 1.9 K. The solid line, arbitrarily drawn through the data, divides the plane into regions which are stable and unstable to the formation of the proposed secondary flow. The dashed lines represent isotherms for $T = 1.4$, 1.6, and 1.8 K, as discussed in the text.

should produce dramatic effects in the vortex line noise spectrum.[19]

We are grateful to F. Moss, J. A. Northby, W. F. Vinen, and R. J. Donnelly for valuable discussions of this problem, and to R. J. Donnelly for communication of experimental results prior to publication.

---

[1]R. K. Childers and J. T. Tough, Phys. Rev. Lett. 31, 911 (1973).

[2]R. K. Childers and J. T. Tough, Phys. Rev. Lett. 35, 527 (1975).

[3]R. K. Childers and J. T. Tough, Phys. Rev. B 13, 1040 (1976).

[4]H. Hoch, L. Busse, and F. Moss, Phys. Rev. Lett. 34, 384 (1975).

[5]D. M. Sitton and F. Moss, Phys. Rev. Lett. 29, 542 (1972).

[6]R. A. Ashton and J. A. Northby, Phys. Rev. Lett. 30, 1119 (1973).

[7]W. F. Vinen, Proc. R. Soc. A 242, 493 (1957).

[8]J. T. Tough, Phys. Rev. 144, A186 (1966).

[9]H. E. Hall and W. F. Vinen, Proc. R. Soc. A 238, 215 (1956).

[10]W. F. Vinen, Proc. R. Soc. A 243, 400 (1957).

[11]L. D. Landau and E. M. Lifshitz, Fluid Mechanics (Pergamon, London, 1959), p. 102.

[12]J. P. Gollub and M. H. Freilich, Phys. Rev. Lett. 33, 1465 (1974).

[13]R. J. Donnelly, Phys. Rev. Lett. 10, 282 (1963).

[14]Since there appears to be no unique way to define $\dot{Q}_c$, it also is allowed to vary over a narrow range. See Table I.

[15]J. T. Tough, W. D. McCormick, and J. G. Dash, Phys. Rev. 140, A1524 (1965).

[16]R. J. Donnelly, F. Reif, and H. Suhl, Phys. Rev. Lett. 9, 363 (1962); R. J. Donnelly, Proc. R. Soc. A 281, 130 (1964).

[17]C. E. Oberly and J. T. Tough, J. Low Temp. Phys. 7, 223 (1972).

[18]For a recent example, see, Robert Graham, Phys. Rev. Lett. 31, 1479 (1973).

[19]R. J. Donnelly (private communication) has recently observed such effects. A strong peak appears in the noise spectrum at high heat currents.